

DEFORMACIJSKA ANALIZA MOSTU RATKOV LAZ PO PELZERJEVI METODI IN METODI IWST

DEFORMATION ANALYSIS OF RATKOV LAZ BRIDGE USING PELZER AND IWST METHOD

Zoran Sušić, Mehmed Batilović, Radovan Đurović, Marko Marković, Marijana Vujinović

UDK: 528.482
Klasifikacija prispevka po COBISS.SI: 1.02
Prispelo: 9. 6. 2023
Sprejeto: 25. 9. 2023

DOI: 10.15292/geodetski-vestnik.2023.04.487-504
REVIEW ARTICLE
Received: 9. 6. 2023
Accepted: 25. 9. 2023

IZVLEČEK

V prispevku je obravnavana uporaba geodetskih metod deformacijske analize armiranobetonskih konstrukcij iz prednapetega betona. Na primeru mostu Ratkov Laz v Črni gori sta uporabljeni dve neodvisni metodi deformacijske analize na podlagi dveh epoh geodetskih meritev v 3D-geodetski mreži, ki je sestavljena iz referenčnega dela mreže in točk na mostu. Analizirani so bili rezultati Pelzerjeve metode (postopka Hannover) in robustne metode IWST. Čeprav so z obema metodama izračunani podobni vektorji pomikov, obstajajo nekatere razlike pri identifikaciji nestabilnih točk na mostu. Z metodo IWST je bilo kot nestabilnih identificiranih precej manj točk kot s Pelzerjevo metodo. Opisani metodi deformacijske analize sta zelo pomembni pri geodetskem opazovanju vseh vrst inženirskih objektov.

ABSTRACT

The paper discusses the application of geodetic methods of deformation analysis of reinforced concrete structures made of prestressed concrete. In the paper, two independent methods of deformation analysis are applied on the example of the Ratkov Laz bridge in Montenegro, based on two epochs of geodetic measurements in a 3D geodetic network, which consists of the reference part of the network and points on the bridge. The results of the Pelzer's method and the robust IWST method were analyzed. Although similar displacement vectors are obtained using the two methods, there are some differences in the identification of unstable points on the bridge. The IWST method identified significantly fewer points as unstable compared to the Pelzer's method. The aforementioned methods of deformation analysis are of great importance in the geodetic observation of all types of engineering facilities.

KLJUČNE BESEDE

deformacijska analiza, robustna metoda IWST, Pelzerjeva metoda, most, elektronski tahimeter

KEY WORDS

deformation analysis, robust IWST method, Pelzer method, bridge, total station

1 INTRODUCTION

The characteristic phases of the construction of concrete bridges refer to the construction of foundations, abutments, coastal and river piers, as well as supporting and roadway construction structures. In addition to the preparatory works, all the mentioned phases must be monitored by geodetic support. A special geodetic micro-network, which consists of the reference part of the network and points on the bridge, is being designed for monitoring the construction of bridges. Bridges represent complex engineering facilities from the geodetic aspect of monitoring their construction. Although geotechnical special sensors, such as precise inclinometers (Xingmin et al., 2005), accelerometers (Olaszek et al., 2020), fiber-optic sensors (Marković et al., 2019), can be used for monitoring purposes, the traditional geodetic method to observing these structures is based on repeated geodetic measurements of horizontal directions, zenith angles and slope distances in geodetic network using conventional or robotic total stations with high performance.

The traditional concept of geodetic deformation measurements of bridges is based on a large number of repeated geodetic measurements, from which quality indicators such as accuracy, reliability, precision and sensitivity of the geodetic micro-network are obtained. The specified parameters can also be obtained in the process of designing geodetic micro-networks for the purposes of monitoring the specified categories of objects, through the procedure of previous estimation of the accuracy and reliability analysis of geodetic measurements and unknown parameters, in the case of 3D point coordinates of the geodetic network. The main task of deformation analysis is the investigation of displacements of an objects in relation to space and time. According to the hierarchy of deformation analysis models, there are congruence and kinematic as descriptive models and static and dynamic, as cause-response models (Heunecke and Welsh, 1999). Although the cause-and-response relationship of the appearance of deformation is often examined nowadays, congruence models are still most often used in deformation analysis procedures in engineering practice (Savšek and Ambrožič, 2023). Congruence models are based on the analysis of two independent measurement epochs.

One of the pioneering methods of Conventional Deformation Analysis (CDA) refers to the Pelzer method or Hanover procedure (Pelzer, 1971). Well-known methods of conventional deformation analysis are the Karlsruhe method (Heck, 1983), Caspary method (Caspary, 1987), Delft method (Heck et al., 1982), Fredericton (Chrzanowski, Chen and Secord, 1982) and others. Research based on these methods can be found in numerous professional and scientific papers (Ambrožič, 2001, 2004; Sušić et al., 2015; Sušić et al., 2017; Vrečko and Ambrožič, 2013). As opposed to CDA, robust deformation analysis methods are based on various robust displacement vector estimation approaches. One of the most well-known robust methods is IWST (Iterative Weighted Similarity Transformation), which was published at the University of New Brunswick in Canada in 1983 (Chen, 1983). Of the recent methods of robust deformation analysis, it is important to mention REDOD and GREDOD methods (Nowel and Kamiński, 2014; Nowel, 2015), a method based of the Hodges–Lehmann estimates, which belong to the class of R-estimates (Duchnowski, 2013), the method based on M-split estimation (Duchnowski and Wyszowska, 2022), a modified IWST and GREDOD method (Batilović et al., 2021, 2022a, 2022b). Testing the efficacy of the CDA method can be measured through the MSR (the mean success rate) factor (Hekimoglu et al., 2010). In the modified method according to the Munich approach, it is proposed to determine the congruence of all lengths and all angles in the network between two epochs of measurement as well as determine the congruence of all triangles between points in the network (Savšek and Ambrožič, 2023).

2 MOTIVATION AND RESEARCH AREA

The subject of geodetic monitoring in this paper refers to the reinforced concrete bridge Ratkov Laz made of prestressed concrete in Montenegro. The bridge is located on the highway Podgorica - Mateševo, section Smokovac - Uvač, in the locality Ratkov Laz ($42^{\circ}36'38.62''$ degrees north latitude and $19^{\circ}23'57.83''$ degrees east longitude). The section from Smokovac to Mateševo is part of the Bar-Boljare Highway, which is part of the Trans-European Motorway (TEM) route through Montenegro. It connects the main route of the TEM (from Gdańsk to Athens and Istanbul) with the Adriatic Sea and it is part of the Belgrade-South Adriatic highway corridor via the TEM.

The bridge spans the valley with a length of about 352 metres and a maximum depth of about 35 metres. The total length of the bridge in the left lane of the highway is 350 metres, and 325 metres in the right lane. The left structure is placed on 2 coastal and 12 central pillars and the right one is placed on 2 coastal and 11 central pillars. The bridge is mostly in a circular curve (Figure 1).



Figure 1: An example of stabilization of reference network points and points on the Ratkov Laz bridge piers

The characteristic phases of the observation of this bridge were related to the installation of foundations, piers, supporting construction structure of the bridge, removal of scaffolding and laying the final layer of asphalt. The subject of this paper refers to the analysis of two epochs of measurement, the zero and the control epoch. The zero epoch was performed after removing the scaffolding from the bridge, while the control epoch was performed after placing the final layer of asphalt on the structure. The zero epoch was carried out during October 2020, while the control epoch was carried out during December 2021. The locations where geodetic observation points are set up refer to the following:

- two benchmarks at the top and at the bottom of central piers at opposite sides whose height is greater than 20 meters;

- two benchmarks at the top of central piers whose height is less than 20 meters;
- two benchmarks in the middle of each span of the bridge;
- two points at the top on abutments.

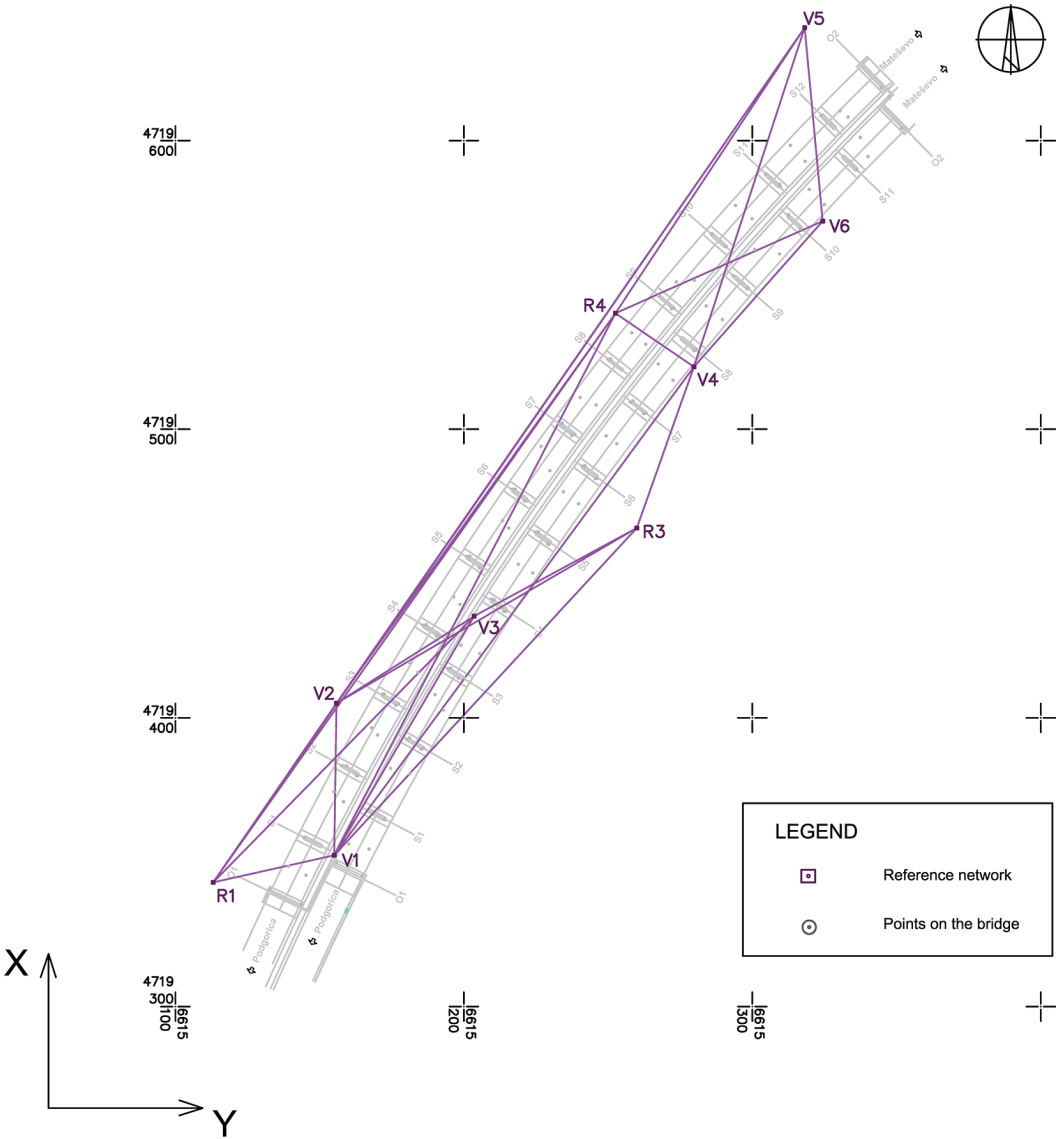


Figure 2: Sketch of the reference geodetic network for bridge monitoring with the disposition of observation points

The total number of points for geodetic monitoring of the Ratkov Laz bridge is 137 (71 for the left lane and 66 for the right lane), which is a sufficient number of points for the geometric interpretation of the bridge in a spatial sense, based on of which high-quality geodetic deformation measurements with deformation analysis can be performed. The reference geodetic network is shown in Figure 2. The locations of the reference points are directly determined by the terrain and object configuration.

3 DATA AND METHODS

The geodetic micro-network consists of a reference part, which is conditionally stable and is mostly placed outside the zone of influence of the bridge and the benchmark points on the bridge that are subject of geodetic monitoring. The total number of points of the reference part of the geodetic network is 9. The geometry of the geodetic network is adapted to the bridge and depends on the terrain configuration. All points on the bridge can be observed from at least two, and mostly three points of the reference part of the geodetic network. The measured quantities in the network are horizontal directions, zenith angles and slope distances. Measurements were performed by the gyrus method in two repetitions. Measurements were made with a total station Leica TS11 that has the following performance: standard deviation of horizontal directions is 1" and standard deviation of measured distances is 1 mm + 1 ppm [mm]. During the measurement, the temperature and atmospheric pressure were taken into account, after which the atmospheric correction was calculated in the postprocessing. The average distance from the points of the reference part of the geodetic micro-network and the points on the bridge is less than 70 meters. The observation plan was identical in both measurement epochs. Adjustment of measurement in both epochs was performed by Least Squares method with the datum definition of the minimum trace to the points of the reference part of the network. Table 1 shows average statistical indicators of the geodetic network in both measurement epochs. All the data listed in table 1 were calculated in the specially projected software package MatGeo in the framework of the Matlab programme, which has been developed in the internal surroundings of the Faculty of Technical Sciences in Novi Sad.

Table 1: Average statistical quality indicators of geodetic network in both measurement epochs

Average statistical quality indicators	Zero epoch	Control epoch
Standard deviation of spatial positions [mm]	1.1	1.3
Internal reliability coefficients for horizontal directions, slope distances and zenith angles, respectively	0.3; 0.8; 0.4	0.3; 0.7; 0.4
Elements of the error ellipsoid (A, B, C) for probability 1-α = 0.95 [mm]	2.8; 1.0; 1.2	3.3; 1.2; 1.4
Minimale detectable deformation in the direction of the semi-major axis for Y and X axis [mm]	2.6; 3.0	3.1; 3.6
Minimale detectable deformation in the direction of the semi-minor axis for Y and X axis [mm]	1.3; 1.1	1.5; 1.3
Minimale detectable deformation in the direction of vertical Z axis	1.7	2.1

The homogeneity of accuracy in both epochs was confirmed, which is a prerequisite for the application of deformation analysis methods. Two representative methods of deformation analysis, Pelzer's and IWST methods, were applied in the paper, after which the results of the two methods were compared.

3.1 Pelzer's method (Hannover approach)

One of the pioneering CDA methods is the Pelzer's method or the Hanover approach, which was published by Pelzer in 1971. The first step in this method is to examine the homogeneity of accuracy in both epochs. After that, the unified variance is calculated based on the following expression:

$$\hat{\sigma}_0^2 = \frac{f_1 \hat{\sigma}_{0_1}^2 + f_2 \hat{\sigma}_{0_2}^2}{f}, \tag{1}$$

where f_1 and f_2 are numbers of freedom degrees in zero and control measurement epoch, $\hat{\sigma}_{0_1}^2$ and $\hat{\sigma}_{0_2}^2$ are *a posteriori* variances at the zero and control epochs, respectively, with $f = f_1 + f_2$ number of degrees of freedom.

In the next step, network congruence is tested using mathematical statistics testing methods. The test statistic of the global congruence point position test is formed:

$$T = \frac{\theta^2}{\hat{\sigma}_0^2} \sim F_{1-\alpha, b, f}, \tag{2}$$

where is the probability $1 - \alpha = 0.95$, b is the rank of the coordinate difference cofactor matrix \mathbf{Q}_d and θ^2 is average non-fitting, which contains information displacements of points, is calculated using the expression:

$$\theta^2 = \frac{\mathbf{d}^T \mathbf{Q}_d^+ \mathbf{d}}{b}, \tag{3}$$

where $\mathbf{d} = \hat{\mathbf{x}}_2 - \hat{\mathbf{x}}_1$ is vector of coordinate differences, $\hat{\mathbf{x}}_1$ and $\hat{\mathbf{x}}_2$ represent vectors of unknown parameters obtained from Least Squares estimates at individual epochs, \mathbf{Q}_d^+ is pseudo-inversion of coordinate differences cofactor matrix, and b is rank of the coordinate differences cofactor matrix $\mathbf{Q}_d^+ = \mathbf{Q}_{\hat{\mathbf{x}}_1} + \mathbf{Q}_{\hat{\mathbf{x}}_2}$, $\mathbf{Q}_{\hat{\mathbf{x}}_1}$ and $\mathbf{Q}_{\hat{\mathbf{x}}_2}$ are cofactor matrices from both individual epochs. If it is valid $T \leq F_{1-\alpha, b, f}$, the hypothesis about the congruence of the positions of the points from the two epochs is not being rejected and the deformation analysis procedure ends there. If it is not valid, the null hypothesis is rejected, i.e. there is at least one unstable (displaced) point in the network.

In that case, the network is divided into two subvectors, one belonging to the points of the reference part of the network (S designates) and the other to the points on the object (O designates). Vector of the coordinate differences \mathbf{d} and the pseudo-inversion of coordinate differences cofactor matrix \mathbf{Q}_d^+ are decomposed as follows (Pelzer, 1971; Ambrožič, 2001; Sušić et al., 2015):

$$\mathbf{d} = \begin{bmatrix} \mathbf{d}_S \\ \mathbf{d}_O \end{bmatrix} \quad \mathbf{Q}_d^+ = \mathbf{P}_d = \begin{bmatrix} \mathbf{P}_{SS} & \mathbf{P}_{SO} \\ \mathbf{P}_{OS} & \mathbf{P}_{OO} \end{bmatrix}. \tag{4}$$

Then the quadratic form $\mathbf{d}^T \mathbf{Q}_d^+ \mathbf{d}$ can be decomposed into the first part related to the non-fitting of the reference part of the network, and the second to the non-fitting of points on the object, where average non-fitting is:

$$\theta_S^2 = \frac{\mathbf{d}_S^T \bar{\mathbf{P}}_{SS} \mathbf{d}_S}{h_S}, \tag{5}$$

where $\bar{\mathbf{P}}_{SS} = \mathbf{P}_{SS} - \mathbf{P}_{SO} \mathbf{P}_{OO}^{-1} \mathbf{P}_{OS}$ and h_S is a rank of $\bar{\mathbf{P}}_{SS}$ (Pelzer, 1971; Ambrožič, 2001; Sušić et al., 2015).

If it is valid $T = \frac{\theta_S^2}{\hat{\sigma}_0^2} \leq F_{1-\alpha, b_S, f}$ zero hypothesis is not being rejected, i.e. reference network points are congruent in two epochs or otherwise, at least one point is unstable. Now the approach is to find the unstable reference points. The procedure of localization of unstable (displaced) points of the reference

part of the network is approached in such a way that the coordinate difference evaluation vector is divided into two subvectors:

$$\mathbf{d}_S = \begin{bmatrix} \mathbf{d}_F \\ \mathbf{d}_B \end{bmatrix}, \quad \bar{\mathbf{P}}_{SS} = \begin{bmatrix} \mathbf{P}_{FF} & \mathbf{P}_{FB} \\ \mathbf{P}_{BF} & \mathbf{P}_{BB} \end{bmatrix}, \tag{6}$$

where the label F refers to conditionally stable points, and the label B refers to conditionally unstable (suspected) points. The decomposition of the quadratic form is carried out as in the previous expressions:

$$\mathbf{d}_S^T \bar{\mathbf{P}}_{SS} \mathbf{d}_S = \mathbf{d}_F^T \bar{\mathbf{P}}_{FF} \mathbf{d}_F + \bar{\mathbf{d}}_B^T \mathbf{P}_{BB} \bar{\mathbf{d}}_B, \tag{7}$$

where

$$\bar{\mathbf{d}}_B = \mathbf{d}_B + \mathbf{P}_{BB}^{-1} \mathbf{P}_{BF} \mathbf{d}_F, \quad \bar{\mathbf{P}}_{FF} = \mathbf{P}_{FF} - \mathbf{P}_{FB} \mathbf{P}_{BB}^{-1} \mathbf{P}_{BF}. \tag{8}$$

Average non-fitting is calculated for all k points of the reference part of the network:

$$\theta_j^2 = \frac{\bar{\mathbf{d}}_B^T \mathbf{P}_{BB_j} \bar{\mathbf{d}}_{B_j}}{h_{B_j}}, \quad (j = 1, 2, \dots, k), \tag{9}$$

where h_{B_j} is a rank of \mathbf{P}_{BB_j} and k is the number of reference points in the network.

The reference point, which has the maximum average non-fitting θ_j^2 , is declared unstable and further testing is conducted without it. $\theta_{REST}^2 = \frac{\mathbf{d}'_F \mathbf{P}_{FF} \mathbf{d}_F}{h_F} = \frac{\mathbf{d}'_F \mathbf{P}_{FF} \mathbf{d}_F}{\text{rank} \bar{\mathbf{P}}_{FF}}$ and test statistic $T = \frac{\theta_{REST}^2}{\hat{\sigma}_0^2}$ are also calcu-

lated. Testing on the remaining points continues until the hypothesis of the congruence of the reference points $T \leq F_{1-\alpha, h_F, f}$ is not being rejected.

In the next step, unstable (displaced) points on the object are localized, which represents the last phase of the analysis. The decomposition of the displacement vector is performed in a similar way as in the previous expressions, where the first subvector contains stable reference points, while the second subvector contains points on the object and unstable reference points. The complete mathematical model of Pelzer's method is presented in a large number of papers (Pelzer, 1971; Ambrožić, 2001; Sušić et al., 2015).

3.2 IWST robust method

The IWST method of deformation analysis is a well-established method that is often used in scientific research. This method has been implemented in several projects of observation of complex objects in practice, the most famous of which is the "Tevatron" accelerator within the Fermilab laboratory in the USA (not operational since 2011).

The IWST method consists of three steps. In the first step, the independent adjustment of measurements of the zero and control epoch is performed using the Least Squares method, where it is a free geodetic network. A detailed explanation of the free adjustment within the Least Squares method can be found in the literature (Tan, 2015). Also, in this step, the procedure of detecting outliers in observations using conventional tests (Data snooping test and τ test) or robust methods (L1 norm, Danish method, and others) is conducted.

The second step involves a robust S transformation of the displacement vector of the network points. The vector $\hat{\mathbf{x}}_2$ is transformed into the datum of vector $\hat{\mathbf{x}}_1$ in order to define a single datum. This task consists of fitting the vector $\hat{\mathbf{x}}_2$ into the vector $\hat{\mathbf{x}}_1$ by reducing it to the center of gravity of the network. The transformed vector takes the following form:

$$\hat{\mathbf{x}}'_2 = \hat{\mathbf{x}}_2 - \mathbf{H}\mathbf{t}, \tag{10}$$

where \mathbf{t} is a vector of parameters of the S transformation and \mathbf{H} is a well-known design matrix of the S transformation in a common datum (Nowel and Kamiński, 2014; Batilović et al., 2021):

$$\mathbf{S} = \mathbf{I} - \mathbf{H}(\mathbf{H}^T\mathbf{W}\mathbf{H})^{-1}\mathbf{H}^T\mathbf{W}, \tag{11}$$

where \mathbf{I} is the identity matrix, and \mathbf{W} weight matrix, which in the first iteration is identical to the identity matrix.

The deformation model is as follows:

$$\mathbf{d} = \hat{\mathbf{x}}'_2 - \hat{\mathbf{x}}_1 = (\hat{\mathbf{x}}_2 - \hat{\mathbf{x}}_1) - \mathbf{H}\mathbf{t}. \tag{12}$$

Optimization problem IWST method is formed by the deformation model (12) and the objective function:

$$\psi(\mathbf{t}) = \|\mathbf{d}\|_1 = \sum |d_i| = \min. \tag{13}$$

The optimization problem is solved numerically using the Iterative Reweighted Least Squares (IRLS) method:

$$\left. \begin{aligned} \hat{\mathbf{d}}^{(k)} &= \mathbf{S}^{(k)}(\hat{\mathbf{x}}_2 - \hat{\mathbf{x}}_1) \\ \mathbf{Q}_{\hat{\mathbf{d}}}^{(k)} &= \mathbf{S}^{(k)}(\mathbf{Q}_{\hat{\mathbf{x}}_1} + \mathbf{Q}_{\hat{\mathbf{x}}_2})(\mathbf{S}^{(k)})^T \\ \mathbf{W}^{(k+1)} &= \text{diag}(\dots, w_{PRP,i}^{(k+1)}, \dots, w_{O,i}, \dots) \end{aligned} \right\}_{k=1,2,\dots}, \tag{14}$$

where $\mathbf{S}^{(k)}$ is the S transformation matrix, $\mathbf{W}^{(k+1)}$ is the weight matrix and k is the iteration number.

In the first iteration of the transformation ($k = 1$) the weight matrix is the identity matrix ($\mathbf{W} = \mathbf{I}$). In the next iterations the weights of the reference network points are determined on the following expression:

$$w_{PRP,i}^{(k+1)} = \frac{1}{\left(|\hat{d}_1^{(k)}| + c\right)}, \tag{15}$$

where $\hat{d}_1^{(k)}$ is the corresponding component of the displacement vector, and c is a small constant value that prevents the occurrence of zero in the denominator. The weights of the object points $w_{O,i}$ are equal to zero, because only reference points participate in the optimization process. In the third step, the stability of network points is tested, i.e. it is examined whether the estimated displacement vectors of individual points are the result of a real displacement or of random measurement errors. For this reason, the following hypotheses are posed:

$$H_0 : E(\hat{\mathbf{d}}_i) = 0 \quad \text{versus} \quad H_a : E(\hat{\mathbf{d}}_i) \neq 0 \tag{16}$$

where $\hat{\mathbf{d}}_i$ is displacement vector of arbitrary points and E mathematical expectation operator. Stability testing of points is performed using a single-point test:

$$T_i = \frac{\hat{\mathbf{d}}_i^T \mathbf{Q}_{\hat{\mathbf{d}}_i} \hat{\mathbf{d}}_i}{\hat{\sigma}_0^2} \sim F_{1, h_i, f} \tag{17}$$

where $\hat{\mathbf{d}}_i$ is the displacement vector, $\mathbf{Q}_{\hat{\mathbf{d}}_i}$ is cofactor matrix of the displacement vector, h_i is a rank of $\mathbf{Q}_{\hat{\mathbf{d}}_i}$, f is the unified number of degrees of freedom, $\hat{\sigma}_0^2$ is the unified *a posteriori* dispersion factor, α_i represents the local level of significance, which is determined depending on the global level of significance α by the well-known expression (Casparly, 1987):

$$\alpha_i = 1 - (1 - \alpha)^{1/m}, \tag{18}$$

where m is number of geodetic network points.

If it is valid $T \leq F_{1-\alpha_i, h_i, f}$ the null hypothesis is not rejected, and the point can be regarded as stable. When $T > F_{1-\alpha_i, h_i, f}$, the null hypothesis is rejected, and it can conclude that the point is significantly displaced. A complete mathematical model of the IWST method with applications in geodetic deformation analysis can be found in numerous literature (Chen, 1983; Nowel, 2014, 2015, 2016; Batilović et. al., 2021).

4 ANALYSIS OF RESULTS AND DISCUSSION

Analysis of the congruence of the reference network using the Pelzer method showed that 4 points are stable and 5 are unstable. Statistical stability was confirmed at the following reference points: R4, V3, V4 and V5, where is the value of the test statistic and the average non-fitting:

$$T = 1.792 \leq F_{0.99, 12, 955} = 2.209, \quad \theta^2_{REST} = 2.442.$$

Analysis of the congruence of the reference network using the IWST method showed that 7 points are stable and 2 are unstable. Statistical stability was confirmed at the following reference points: R1, R4, V2, V3, V4, V5 and V6. Localization of points on the bridge using the Pelzer method showed that 26 points on the bridge were identified as statistically stable, while the remaining 111 points were significantly unstable.

Localization of points on the bridge using the IWST robust method showed that 65 points on the bridge were identified as statistically stable, while the remaining 72 points were significantly displaced (Appendix 1). The average intensity of the displacement vector in the horizontal plane for all points on the bridge is 6.7 mm using the Pelzer method, while it is 6.6 mm using the IWST method. The displacement intensities for characteristic points with higher displacement intensities along all three axes (Y , X and H) are shown for both methods (Pelzer and IWST) in Table 2. Also, the table 2 shows the values of the average non-fitting θ^2 (eq. 9) for the Pelzer's method, as well as the value of the test statistic T (eq. 17) and the value of Fisher's distribution F for each point in the IWST method. The complete displacement results at all points on the bridge are shown in Appendix 1.

Table 2: Results of deformation analysis using the Pelzer method (CDA) and the IWST (robust) method for reference points of the geodetic network and characteristic points on the bridge

Points	Pelzer - Intensity of displacements [mm]						IWST- Intensity of displacements [mm]				
	Status	θ^2	dY	dX	dH	T	F	Status	dY	dX	dH
Reference points of the geodetic network											
R1	Unstable	3586.3	7.5	7.9	0.8	3.3	6.2	Stable	0.4	0.9	-1.3
R3	Unstable	3518.3	-6.6	-6.8	-1.0	19.2	6.2	Unstable	0.7	0.2	2.4
R4	Stable	1.9	0.3	0.4	-0.3	0.2	6.2	Stable	-0.1	-0.5	-0.1
V1	Unstable	553.7	-0.6	3.1	-1.1	7.3	6.2	Unstable	0.0	2.4	-0.4
V2	Unstable	39.1	0.5	0.5	-1.6	4.2	6.2	Stable	0.2	0.0	1.3
V3	Stable	2.7	-0.9	-0.2	-0.1	1.8	6.2	Stable	-1.0	-0.1	0.4
V4	Stable	3.3	-0.4	-0.8	-0.1	1.3	6.2	Stable	-0.6	-1.2	0.0
V5	Stable	2.5	-0.2	-0.6	0.4	1.7	6.2	Stable	0.1	-1.0	0.6
V6	Unstable	165.8	-0.7	2.7	2.0	1.2	6.2	Stable	-0.5	0.5	-0.2
Points on bridge spans											
LL1	Unstable	3768.2	-11.0	-21.7	3.2	312.5	6.2	Unstable	-10.2	-19.4	2.4
LL2	Unstable	216.2	-8.4	-13.9	0.5	123.3	6.2	Unstable	-9.1	-13.2	0
LL3	Unstable	1432.8	-6.8	-11.5	2.1	654.1	6.2	Unstable	-8.1	-11.3	1.6
LL4	Unstable	135.8	-5.9	-9.2	2.1	86	6.2	Unstable	-7.0	-9.5	2
LL12	Unstable	85.6	9.4	10.1	-0.9	53.4	6.2	Unstable	9.5	9.5	-0.4
LL13	Unstable	404.5	9.8	10.3	0.1	120.9	6.2	Unstable	9.7	9.6	0.6
LR1	Unstable	2211.4	-4.8	-17.6	3.1	185.8	6.2	Unstable	-6.4	-16.3	1.7
LR2	Unstable	335.8	-6.8	-14.5	-0.1	168.2	6.2	Unstable	-7.8	-14.5	0.2
LR3	Unstable	1029.7	-7.1	-11.5	2.2	508.3	6.2	Unstable	-8.3	-11.3	1.8
LR12	Unstable	543.2	9.2	6.4	-1.9	111.6	6.2	Unstable	9.1	5.6	-1.5
LR13	Unstable	80.2	8.1	6.6	0.2	34.7	6.2	Unstable	8.0	5.9	0.6
RL1	Unstable	163	-8.9	-16.5	1.3	77.2	6.2	Unstable	-9.2	-15.9	0.2
RL2	Unstable	77.7	-7.2	-13.2	1.6	40.9	6.2	Unstable	-8.3	-13.5	1.5
RL3	Unstable	143.8	-5.0	-9.1	1.7	100.4	6.2	Unstable	-5.8	-9.3	2.0
RL4	Unstable	36	-5.5	-7.0	2.1	25.7	6.2	Unstable	-6.3	-7.1	2.4
RL10	Unstable	151.3	6.1	8.1	0.7	23.8	6.2	Unstable	6.1	7.4	0.8
RL11	Unstable	1527.8	7.6	8.8	-1.5	91.1	6.2	Unstable	7.4	8.0	-1.0
RL12	Unstable	248.9	9.5	10.5	-0.2	90.2	6.2	Unstable	9.5	9.7	0.2
RR1	Unstable	204.9	-6.4	-16.2	1.9	114.7	6.2	Unstable	-7.3	-15.6	1.3
RR2	Unstable	78.3	-5.0	-11.9	1.7	36	6.2	Unstable	-5.9	-12.1	1.6
RR3	Unstable	15.8	-4.4	-9.0	1.3	11	6.2	Unstable	-5.3	-9.2	1.6
RR4	Unstable	38.4	-2.7	-7.3	1.8	25.8	6.2	Unstable	-3.5	-7.5	2.1
RR10	Unstable	157.9	7.2	8.2	1.1	39.3	6.2	Unstable	7.1	7.4	1.3
Points on the tops of the pillars											
LS21	Unstable	383.4	-7.1	-13.2	1.7	179.5	6.2	Unstable	-7.8	-14	2.5
LS23	Unstable	141	-7.5	-13.5	1.8	83.7	6.2	Unstable	-8.6	-14.1	1.6
LS31	Unstable	49.8	-6.2	-11.1	1.4	25.3	6.2	Unstable	-7.1	-11.1	1.7

Points	Pelzer - Intensity of displacements [mm]						IWST- Intensity of displacements [mm]				
	Status	θ^2	dY	dX	dH	T	F	Status	dY	dX	dH
LS33	Unstable	30.5	-6.8	-12.3	1.5	22.4	6.2	Unstable	-7.7	-12.4	1.8
LS41	Unstable	305.1	-3.9	-7.2	-0.2	56.2	6.2	Unstable	-5.9	-7.4	1.6
LS43	Unstable	52.7	-7.1	-7.9	2.4	37.1	6.2	Unstable	-7.9	-8.1	2.7
LS93	Unstable	62.6	9.5	12.4	2.8	31.7	6.2	Unstable	9.3	11.9	2.7
RS21	Unstable	202.7	-4.6	-9.8	2.0	138.5	6.2	Unstable	-5.8	-9.8	1.9
RS23	Unstable	18.1	-3.7	-9.0	0.1	10.9	6.2	Unstable	-4.7	-9.1	0.5
RS31	Unstable	54.9	-2.9	-6.8	2.6	38.3	6.2	Unstable	-3.7	-7.0	2.9

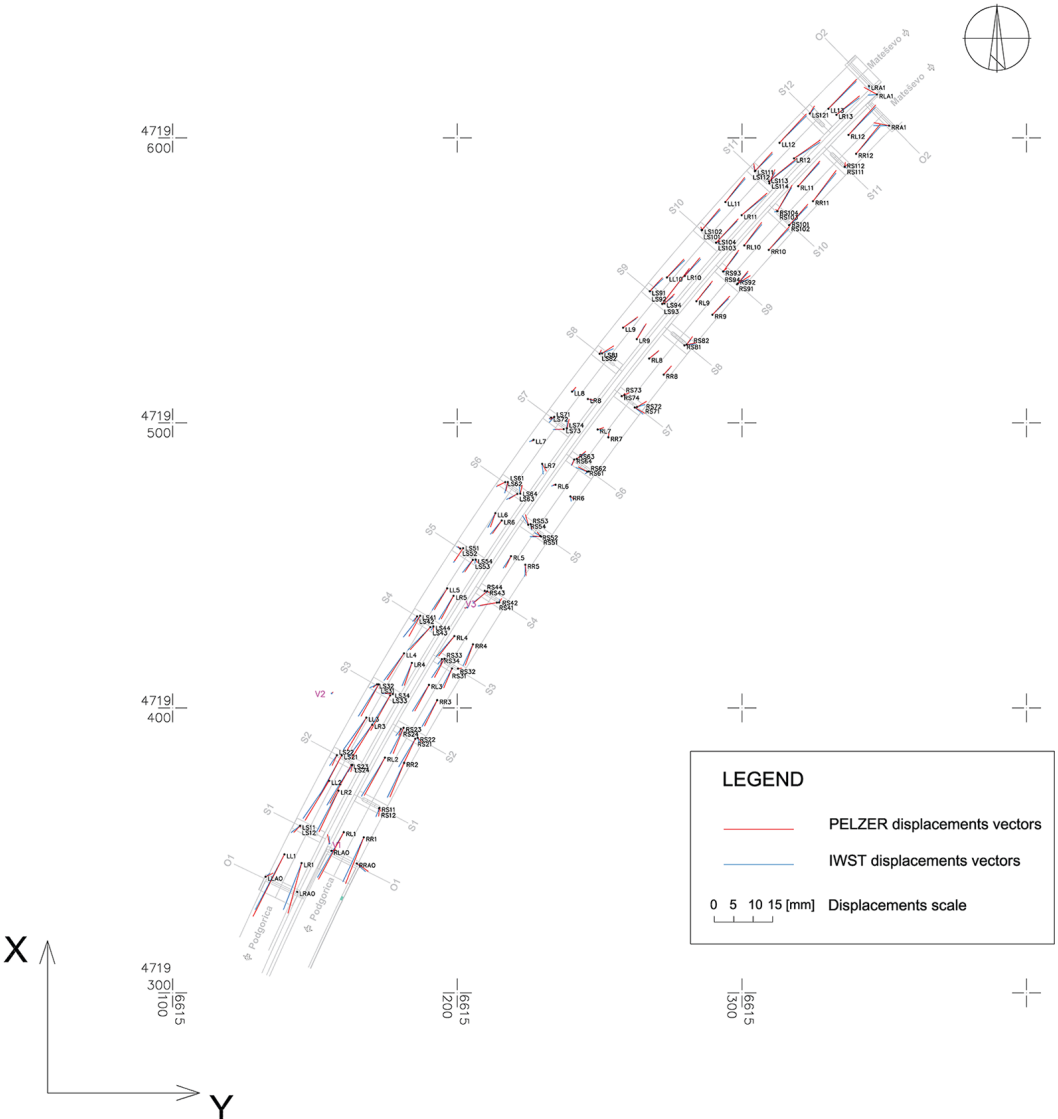


Figure 3: Sketch of the geodetic network of the Ratkov Laz bridge with Pelzer and IWST displacement vectors

As can be seen from Figure 3, the interpretation of the displacement vector for points on the bridge is similar in both deformation analysis methods. The points located at the top of the pillars (from pillar S1 to pillar S4), as well as the points on the spans between these pillars show significant movements with the azimuth of the displacement in the southwestern direction of the road towards Podgorica. Displacements range is from 10 to over 15 mm. It is important to point out the different influence of temperature on measurements in zero and control epochs. Most of the points on the pillars in the middle of the bridge (from pillar S4 to pillar S9) are generally statistically evaluated as stable by applying the IWST robust method. The points located at the top of the pillars on the north side of the bridge (from pillar S10 to pillar S12), as well as the points on the spans between these pillars show significant movements with the azimuth of the displacement in the northeastern direction of the road towards Mateševo. The displacement intensities are similar to those on the southern side of the bridge (from 10 to over 15 mm), while the displacement azimuths are oriented in the opposite direction compared to the southern side of the bridge.

5 CONCLUSION

Monitoring during the construction and exploitation of traffic infrastructure facilities, especially bridges, includes the traditional and modern approach of geodetic observation. If the engineering facilities during construction are affected by factors such as wind, sun radiation, the influence of cranes, etc., it is important to consider the use of continuous GNSS measurements in combination with special geotechnical sensors (inclinometers, extensometers, etc). However, in a large number of cases in engineering practice, an important segment is traditional geodetic monitoring approach using total stations (conventional or robotized) in the process of periodic geodetic monitoring.

The paper presents an example from the practice of geodetic monitoring of the Ratkov Laz bridge on the highway in Montenegro, whose stability is assessed by models of the congruence of the geodetic network in individual measurement epochs. For the purpose of applying the deformation analysis of two epochs of measurement, representative methods from the group of CDA (Pelzer's) and robust methods (IWST) were used. The intensities and azimuths of the displacement vectors showed similar results for both methods. However, the conclusions about the statistical stability/instability of certain points on the bridge, showed significant differences. A significantly smaller number of points on the bridge were evaluated as statistically stable with the Pelzer's method compared to the IWST method. By applying the IWST method, more objective results were obtained, considering the practical significance of moving points on the bridge. The results of displacements of the points on the top of the pillars on the south and north sides of the bridge showed the opposite direction of displacements and similar intensities of displacements, while the points on the central part of the bridge were generally assessed as stable by applying the IWST method. It is known that numerous modifications of the IWST method are available in the scientific literature, which differ from each other in the use of the optimization condition of robust estimation, i.e. objective functions (Huber's, Danish, etc). Testing the efficacy of different weight functions can be examined using the MSR factor (Hekimoglu et al., 2010; Sušić et al., 2017), which was not the subject of research in this paper.

Although the interpretation of the displacement vector is interesting both from a geodetic and construction point of view, the main focus of the paper is on the comparative research of conventional and robust methods of deformation analysis, which have their role in geodetic observation of all kinds of engineering facilities. When considering the conclusions from the analysis of the stability of points, and bearing in mind the practical importance of the displacement of points on the bridge, it is concluded that the IWST method gives more objective results that correspond more closely to the real situation compared to the Pelzer's method.

Acknowledgement

The research has been conducted within the project "Scientific theoretical and experimental research and improvement of educational process in the field of civil engineering", developed at the Department of Civil Engineering and Geodesy, Faculty of Technical Sciences, University of Novi Sad, Serbia.

Literature and references:

Ambrožič, T. (2004). Deformacijska analiza po postopku Karlsruhe. *Geodetski vestnik*, 48 (3), 315–331

Ambrožič, T. (2001). Deformacijska analiza po postopku Hannover. *Geodetski vestnik*, 45 (1&2), 38–53

Batilović, M., Đurović, R., Sušić, Z., Kanović, Ž., Cekić, Z. (2022a). Robust estimation of deformation from observation differences using some evolutionary optimisation algorithms. *Sensors*, 22 (1), 159, 1–26. DOI: <https://doi.org/10.3390/s22010159>

Batilović, M., Kanović, Ž., Sušić, Z., Bulatović, V. (2022b). Deformacijska analiza po modificirani metodi GREDOD. | Deformation analysis: the modified GREDOD method. *Geodetski vestnik*, 66 (1), 60–75. DOI: [10.15292/geodetski-vestnik.2022.01.60-75](https://doi.org/10.15292/geodetski-vestnik.2022.01.60-75)

Batilović, M., Sušić, Z., Kanović, Ž., Marković, M.Z., Vasić, D., Bulatović, V. (2021). Increasing efficiency of the robust deformation analysis methods using genetic algorithm and generalised particle swarm optimisation. *Survey Review*, 53, 378, 193–205. DOI: [10.1080/00396265.2019.1706294](https://doi.org/10.1080/00396265.2019.1706294)

Caspary, W.F. (1987). *Concepts of Network and Deformation Analysis*. Kensington: The University of New South Wales, School of Surveying, Australia.

Chen, Y.Q. (1983). Analysis of deformation surveys – a generalized method. Technical Report. Frederickton: UNB Geodesy and Geomatics Engineering. University of New Brunswick.

Chrzanowski, A., Chen, Y.Q., Secord, J.M. (1982). A Generalized Approach to the Geometrical Analysis of Deformation Surveys. In 3rd International Symposium on Deformation Measurements by Geodetic Methods. 25–27 August 1982, Budapest, Hungary.

Duchnowski, R. (2013). Hodges–Lehmann estimates in deformation analyses. *Journal of Geodesy* 87:873–884. DOI: [10.1007/s00190-013-0651-2](https://doi.org/10.1007/s00190-013-0651-2)

Duchnowski, R., Wyszowska, P. (2022). Msplit Estimation Approach to Modeling Vertical Terrain Displacement from TLS Data Disturbed by Outliers. *Remote Sensing* 14(21):5620. DOI: [10.3390/rs14215620](https://doi.org/10.3390/rs14215620)

Heck, B. (1983). Das Analyseverfahren Des Geodätischen Instituts Der Universität Karlsruhe Stand 1983, In *Deformationsanalysen '83-Geometrische Analyse und Interpretation von Deformationen Geodätischer Netze*. 22 April 1983, München, Germany.

Heck, B., Kok, J.J., Welsch, W., Baumer, R., Chrzanowski, A., Chen, Y.Q., Secord, J.M. (1982). Report of the FIG Working Group on the Analysis of Deformation Measurements. In 3rd International Symposium on Deformation Measurements by Geodetic Methods. 25–27 August 1982, Budapest, Hungary.

Hekimoglu, S., Erdogan, B., Butterworth, S. (2010). Increasing the Efficacy of the Conventional Deformation Analysis Methods: Alternative Strategy. *Journal of Surveying Engineering* 136(2). DOI: [10.1061/\(ASCE\)SU.1943-5428.0000018](https://doi.org/10.1061/(ASCE)SU.1943-5428.0000018)

Marković, Z.M., Bajić, S.J., Batilović, M., Sušić, Z., Joža, A., Stojanović, M.G. (2019). Comparative Analysis of Deformation Determination by Applying Fiber-optic 2D Deflection Sensors and Geodetic Measurements. *Sensors*, 19 (4), 844, 1–14. DOI: <https://doi.org/10.3390/s19040844>

Nowel, K. (2015). Robust M-Estimation in Analysis of Control Network Deformations: Classical and New Method. *Journal of Surveying Engineering*, 141 (4), 1–10. DOI: [https://doi.org/10.1061/\(ASCE\)SU.1943-5428.0000144](https://doi.org/10.1061/(ASCE)SU.1943-5428.0000144)

Nowel, K. (2016). Investigating efficacy of robust M estimation of deformation from observation differences. *Survey Review*, 48, 346, 21–30, DOI: <http://dx.doi.org/10.1080/00396265.2015.1097585>

Nowel, K., Kamiński, W. (2014). Robust estimation of deformation from observation differences for free control networks. *Journal of Geodesy*, 88 (8), 749–764. DOI: <https://doi.org/10.1007/s00190-014-0719-7>

Olaszek, P., Wyczałek, I., Sala, D., Kokot, M., Świercz, A. (2020). Monitoring of the Static and Dynamic Displacements of Railway Bridges with the Use of Inertial Sensors. *Sensors*, 20 (10), 2767, 1–24. DOI: <https://doi.org/10.3390/s20102767>

Pelzer, H. (1971). *Zur Analyse geodätischer Deformationsmessungen*. München: Deutsche Geodätische Kommission. Reihe C. No. 164

Savšek, S., Ambrožič, T. (2023). Modificirana metoda deformacijske analize po postopku München. Modified method of deformation analysis according to the Munich approach. *Geodetski vestnik*, 67 (2), 131-b164. DOI: [10.15292/geodetski-vestnik.2023.02.131-164](https://doi.org/10.15292/geodetski-vestnik.2023.02.131-164)

Sušić, Z., Batilović, M., Ninkov, T., Aleksić, I., Bulatović, V. (2015). Identification of movements using different methods of deformation analysis. *Geodetski vestnik*, 59 (3), 537–553. DOI: 10.15292/geodetski-vestnik.2015.03.537-553

Sušić, Z., Batilović, M., Ninkov, T., Bulatović, V., Aleksić, I., Nikolić, G. (2017). Geometric deformation analysis in free geodetic networks: case study for Fruška Gora in Serbia. *Acta Geodynamica et Gromaterialia*, 14 (3), 187, 341–355. DOI: 10.13168/AGG.2017.0017

Tan, W. (2015). Inner constraints for 3-D survey networks. *Journal of Spatial Science*.

Taylor & Francis

Vrečko, A., Ambrožič, T. (2013). Deformacijska analiza po postopku Fredericton. *Geodetski vestnik*, 57 (3), 479–497. DOI: <https://doi.org/10.15292/geodetski-vestnik.2013.03.479-497>

Xingmin, H., Xueshan, Y., Qiao, H. (2005). Using Inclinometers to Measure Bridge Deflection. *Journal of Bridge Engineering*, 10 (5), 1–6. DOI: 10.1061/(ASCE)1084-0702(2005)10:5(564)

Appendix 1: Results of deformation analysis using the Pelzer method (CDA) and the IWST (robust) method

Points	Pelzer - Intensity of displacements [mm]						IWST- Intensity of displacements [mm]					
	Status	θ^2	dY	dX	dH	T	F	Status	dY	dX	dH	
R1	Unstable	3586.3	7.5	7.9	0.8	3.3	6.2	Stable	0.4	0.9	-1.3	
R3	Unstable	3518.3	-6.6	-6.8	-1.0	19.2	6.2	Unstable	0.7	0.2	2.4	
R4	Stable	1.9	0.3	0.4	-0.3	0.2	6.2	Stable	-0.1	-0.5	-0.1	
V1	Unstable	553.7	-0.6	3.1	-1.1	7.3	6.2	Unstable	0.0	2.4	-0.4	
V2	Unstable	39.1	0.5	0.5	-1.6	4.2	6.2	Stable	0.2	0.0	1.3	
V3	Stable	2.7	-0.9	-0.2	-0.1	1.8	6.2	Stable	-1.0	-0.1	0.4	
V4	Stable	3.3	-0.4	-0.8	-0.1	1.3	6.2	Stable	-0.6	-1.2	0.0	
V5	Stable	2.5	-0.2	-0.6	0.4	1.7	6.2	Stable	0.1	-1.0	0.6	
V6	Unstable	165.8	-0.7	2.7	2.0	1.2	6.2	Stable	-0.5	0.5	-0.2	
LL1	Unstable	3768.2	-11.0	-21.7	3.2	312.5	6.2	Unstable	-10.2	-19.4	2.4	
LL10	Unstable	66.0	5.9	6.4	0.4	20.3	6.2	Unstable	6.1	6.0	0.5	
LL11	Unstable	17.5	6.8	8.6	1.2	11.3	6.2	Unstable	7.0	8.2	1.4	
LL12	Unstable	85.6	9.4	10.1	-0.9	53.4	6.2	Unstable	9.5	9.5	-0.4	
LL13	Unstable	404.5	9.8	10.3	0.1	120.9	6.2	Unstable	9.7	9.6	0.6	
LL2	Unstable	216.2	-8.4	-13.9	0.5	123.3	6.2	Unstable	-9.1	-13.2	0.0	
LL3	Unstable	1432.8	-6.8	-11.5	2.1	654.1	6.2	Unstable	-8.1	-11.3	1.6	
LL4	Unstable	135.8	-5.9	-9.2	2.1	86.0	6.2	Unstable	-7.0	-9.5	2.0	
LL5	Unstable	34.3	-4.5	-7.4	2.7	23.9	6.2	Unstable	-5.3	-7.6	3.0	
LL6	Unstable	37.8	-1.7	-4.8	1.5	22.2	6.2	Unstable	-2.6	-5.0	1.8	
LL7	Unstable	5.0	-0.6	-0.5	1.9	4.6	6.2	Stable	-1.4	-0.6	2.3	
LL8	Unstable	5.2	1.3	1.5	0.8	1.3	6.2	Stable	1.0	0.5	0.8	
LL9	Unstable	4.6	5.1	3.8	0.6	2.6	6.2	Stable	4.6	3.2	1.1	
LLA1	Unstable	132.8	-12.4	-4.8	-3.2	64.7	6.2	Unstable	-13.6	-6.5	-2.3	
LLAO	Unstable	15.4	2.6	1.3	-0.8	1.9	6.2	Stable	1.6	1.2	-0.4	
LR1	Unstable	2211.4	-4.8	-17.6	3.1	185.8	6.2	Unstable	-6.4	-16.3	1.7	
LR10	Unstable	56.9	5.2	6.3	0.3	14.6	6.2	Unstable	5.5	5.9	0.4	
LR11	Unstable	29.9	8.9	7.7	1.5	17.6	6.2	Unstable	8.6	6.9	1.4	
LR12	Unstable	543.2	9.2	6.4	-1.9	111.6	6.2	Unstable	9.1	5.6	-1.5	
LR13	Unstable	80.2	8.1	6.6	0.2	34.7	6.2	Unstable	8.0	5.9	0.6	
LR2	Unstable	335.8	-6.8	-14.5	-0.1	168.2	6.2	Unstable	-7.8	-14.5	0.2	

Points	Pelzer - Intensity of displacements [mm]						IWST- Intensity of displacements [mm]				
	Status	θ^2	dY	dX	dH	T	F	Status	dY	dX	dH
LR3	Unstable	1029.7	-7.1	-11.5	2.2	508.3	6.2	Unstable	-8.3	-11.3	1.8
LR4	Unstable	145.0	-2.6	-7.9	4.1	95.2	6.2	Unstable	-3.4	-8.0	4.4
LR5	Unstable	36.5	-4.3	-8.0	2.0	24.6	6.2	Unstable	-5.1	-8.2	2.3
LR6	Unstable	22.6	-3.2	-4.5	1.7	13.9	6.2	Unstable	-3.9	-4.8	2.0
LR7	Unstable	11.2	1.4	-2.5	1.8	6.6	6.2	Unstable	0.3	-3.6	1.9
LR8	Unstable	6.2	2.4	-0.5	0.5	1.8	6.2	Stable	1.8	-0.6	0.9
LR9	Unstable	5.6	3.3	5.4	0.7	2.8	6.2	Stable	2.7	4.7	1.0
LRA1	Stable	2.3	0.1	0.0	-1.0	0.5	6.2	Stable	0.1	-1.0	-0.5
LS101	Unstable	16.8	6.3	7.5	0.5	9.5	6.2	Unstable	6.5	7.1	0.7
LS102	Stable	1.6	-0.5	1.0	-0.4	0.3	6.2	Stable	-0.6	0.3	-0.3
LS103	Unstable	49.1	7.8	8.4	1.4	23.6	6.2	Unstable	7.4	7.6	1.4
LS104	Stable	0.6	1.5	0.5	0.0	0.7	6.2	Stable	1.3	-0.2	0.1
LS11	Unstable	5.4	-2.2	-2.3	0.6	4.7	6.2	Stable	-3.1	-2.3	0.9
LS111	Unstable	17.0	5.9	6.5	0.3	11.9	6.2	Unstable	6.0	5.9	0.7
LS112	Stable	3.2	-0.4	2.6	-0.3	0.8	6.2	Stable	-0.4	1.7	0.1
LS113	Unstable	707.1	9.7	7.9	-0.2	76.8	6.2	Unstable	9.4	7.2	0.2
LS114	Unstable	122.0	1.9	4.8	-0.4	8.5	6.2	Unstable	1.9	3.8	-0.1
LS12	Stable	0.4	0.2	-0.4	0.0	0.2	6.2	Stable	-0.7	-0.5	0.3
LS121	Unstable	10.6	1.6	2.6	-1.0	3.4	6.2	Stable	1.6	1.8	-0.4
LS122	Unstable	3.7	-6.4	-11.1	-0.7	3.0	6.2	Stable	-6.6	-12.1	-0.7
LS21	Unstable	383.4	-7.1	-13.2	1.7	179.5	6.2	Unstable	-7.8	-14.0	2.5
LS22	Unstable	16.8	-1.7	-3.5	0.0	13.6	6.2	Unstable	-2.5	-3.6	0.3
LS23	Unstable	141.0	-7.5	-13.5	1.8	83.7	6.2	Unstable	-8.6	-14.1	1.6
LS24	Stable	2.4	-0.6	-2.3	-0.2	1.7	6.2	Stable	-1.5	-2.4	0.1
LS31	Unstable	49.8	-6.2	-11.1	1.4	25.3	6.2	Unstable	-7.1	-11.1	1.7
LS32	Unstable	4.3	-1.4	-1.0	-0.1	2.8	6.2	Stable	-2.5	-1.2	0.2
LS33	Unstable	30.5	-6.8	-12.3	1.5	22.4	6.2	Unstable	-7.7	-12.4	1.8
LS34	Unstable	4.9	-2.8	0.2	0.2	5.1	6.2	Stable	-3.7	0.1	0.5
LS41	Unstable	305.1	-3.9	-7.2	-0.2	56.2	6.2	Unstable	-5.9	-7.4	1.6
LS42	Stable	2.3	-1.0	-1.7	1.1	1.8	6.2	Stable	-1.6	-1.7	1.4
LS43	Unstable	52.7	-7.1	-7.9	2.4	37.1	6.2	Unstable	-7.9	-8.1	2.7
LS44	Unstable	15.5	0.0	-1.4	0.3	1.8	6.2	Stable	-0.8	-1.3	0.7
LS51	Stable	2.4	-3.0	-4.4	-0.1	2.0	6.2	Stable	-3.3	-5.0	-0.1
LS52	Stable	1.7	-0.8	0.7	-1.4	1.1	6.2	Stable	-1.2	0.6	-1.2
LS53	Unstable	9.9	-2.8	-4.2	2.9	8.0	6.2	Unstable	-3.6	-4.4	3.3
LS54	Unstable	8.1	0.7	-1.0	-0.7	0.7	6.2	Stable	-0.3	-1.3	-0.3
LS61	Unstable	7.7	-0.6	-3.0	3.0	5.6	6.2	Stable	-1.1	-3.8	3.0
LS62	Stable	2.2	-2.9	-1.4	0.1	1.6	6.2	Stable	-3.1	-1.6	0.2

Points	Pelzer - Intensity of displacements [mm]						IWST- Intensity of displacements [mm]				
	Status	θ^2	dY	dX	dH	T	F	Status	dY	dX	dH
LS63	Unstable	24.4	-2.9	-1.8	2.8	17.0	6.2	Unstable	-3.8	-2.0	3.2
LS64	Stable	1.4	0.7	2.9	-0.1	1.0	6.2	Stable	-0.3	2.4	0.2
LS71	Stable	3.4	-1.4	-1.0	1.5	2.6	6.2	Stable	-1.8	-1.9	1.5
LS72	Stable	0.5	-0.6	-0.2	0.5	0.3	6.2	Stable	-0.7	-0.5	0.5
LS73	Unstable	6.6	-3.0	0.0	2.1	5.8	6.2	Stable	-3.7	-0.2	2.5
LS74	Unstable	7.6	0.7	3.1	0.4	2.7	6.2	Stable	0.0	3.0	0.7
LS81	Unstable	134.3	4.1	2.7	-0.3	26.3	6.2	Unstable	4.0	1.6	-0.1
LS82	Stable	2.1	0.5	1.3	-0.4	1.0	6.2	Stable	0.4	0.5	-0.5
LS91	Unstable	94.7	4.4	4.8	0.6	16.4	6.2	Unstable	4.7	4.4	0.8
LS92	Stable	2.2	0.6	0.3	0.6	0.9	6.2	Stable	0.5	-0.2	0.5
LS93	Unstable	62.6	9.5	12.4	2.8	31.7	6.2	Unstable	9.3	11.9	2.7
LS94	Unstable	5.0	3.5	3.3	-0.5	1.9	6.2	Stable	3.0	2.4	-0.3
RL1	Unstable	163.0	-8.9	-16.5	1.3	77.2	6.2	Unstable	-9.2	-15.9	0.2
RL10	Unstable	151.3	6.1	8.1	0.7	23.8	6.2	Unstable	6.1	7.4	0.8
RL11	Unstable	1527.8	7.6	8.8	-1.5	91.1	6.2	Unstable	7.4	8.0	-1.0
RL12	Unstable	248.9	9.5	10.5	-0.2	90.2	6.2	Unstable	9.5	9.7	0.2
RL2	Unstable	77.7	-7.2	-13.2	1.6	40.9	6.2	Unstable	-8.3	-13.5	1.5
RL3	Unstable	143.8	-5.0	-9.1	1.7	100.4	6.2	Unstable	-5.8	-9.3	2.0
RL4	Unstable	36.0	-5.5	-7.0	2.1	25.7	6.2	Unstable	-6.3	-7.1	2.4
RL5	Unstable	7.2	-2.0	-4.0	2.1	5.5	6.2	Stable	-2.7	-4.2	2.4
RL6	Unstable	4.6	-0.8	-0.2	2.1	4.1	6.2	Stable	-1.4	-0.5	2.3
RL7	Stable	2.4	2.1	0.6	0.7	1.5	6.2	Stable	1.5	-0.4	0.7
RL8	Unstable	84.3	3.3	2.7	-0.1	13.7	6.2	Unstable	3.1	2.4	-0.3
RL9	Unstable	119.2	5.6	7.0	-0.6	33.1	6.2	Unstable	5.1	6.1	-0.4
RLA1	Unstable	16.5	-4.4	2.5	1.0	11.1	6.2	Unstable	-3.1	-0.2	2.2
RLAO	Unstable	657.7	1.5	0.4	-0.4	6.6	6.2	Unstable	0.6	0.3	0.0
RR1	Unstable	204.9	-6.4	-16.2	1.9	114.7	6.2	Unstable	-7.3	-15.6	1.3
RR10	Unstable	157.9	7.2	8.2	1.1	39.3	6.2	Unstable	7.1	7.4	1.3
RR11	Unstable	53.5	8.1	10.8	-0.4	30.0	6.2	Unstable	8.0	9.8	0.0
RR12	Unstable	183.9	8.5	10.3	-0.8	67.3	6.2	Unstable	8.4	9.5	-0.4
RR2	Unstable	78.3	-5.0	-11.9	1.7	36.0	6.2	Unstable	-5.9	-12.1	1.6
RR3	Unstable	15.8	-4.4	-9.0	1.3	11.0	6.2	Unstable	-5.3	-9.2	1.6
RR4	Unstable	38.4	-2.7	-7.3	1.8	25.8	6.2	Unstable	-3.5	-7.5	2.1
RR5	Unstable	17.4	0.3	-3.9	0.2	7.9	6.2	Unstable	-0.2	-4.1	0.4
RR6	Unstable	4.9	1.3	-0.9	1.6	3.1	6.2	Stable	0.3	-1.7	1.7
RR7	Stable	3.3	0.2	1.3	1.1	1.7	6.2	Stable	-0.2	0.5	1.1
RR8	Unstable	4.3	2.7	3.0	-0.1	1.4	6.2	Stable	2.2	2.3	0.1
RR9	Unstable	74.7	6.0	6.5	0.2	24.6	6.2	Unstable	5.7	5.6	0.5

Points	Pelzer - Intensity of displacements [mm]						IWST- Intensity of displacements [mm]				
	Status	θ^2	dY	dX	dH	T	F	Status	dY	dX	dH
RRA1	Unstable	17.1	-5.3	1.0	1.0	8.9	6.2	Unstable	-5.5	0.0	1.5
RRAO	Unstable	28.2	4.0	-2.7	0.5	2.6	6.2	Stable	3.0	-2.8	0.8
RS101	Unstable	13.9	6.5	7.3	0.7	7.0	6.2	Unstable	6.3	6.5	0.7
RS102	Stable	2.5	3.1	3.1	0.2	1.2	6.2	Stable	2.9	2.3	0.1
RS103	Unstable	1257.3	5.2	9.1	1.1	51.1	6.2	Unstable	5.0	8.2	1.4
RS104	Unstable	7.4	-0.7	0.5	-1.1	1.1	6.2	Stable	-1.1	-0.3	-0.9
RS11	Unstable	28.0	-0.3	-3.0	1.0	7.4	6.2	Unstable	-1.2	-3.1	1.3
RS111	Stable	3.2	0.2	1.6	1.1	1.8	6.2	Stable	-0.1	0.4	1.2
RS112	Stable	1.8	1.0	0.8	-0.3	0.5	6.2	Stable	0.6	-0.4	-0.1
RS12	Unstable	6.6	0.7	-1.0	0.3	1.1	6.2	Stable	-0.2	-1.1	0.6
RS21	Unstable	202.7	-4.6	-9.8	2.0	138.5	6.2	Unstable	-5.8	-9.8	1.9
RS22	Unstable	4.6	1.6	-1.6	-0.6	0.9	6.2	Stable	0.6	-1.8	-0.2
RS23	Unstable	18.1	-3.7	-9.0	0.1	10.9	6.2	Unstable	-4.7	-9.1	0.5
RS24	Stable	1.3	-0.7	-2.2	-0.4	0.6	6.2	Stable	-1.7	-2.3	0.0
RS31	Unstable	54.9	-2.9	-6.8	2.6	38.3	6.2	Unstable	-3.7	-7.0	2.9
RS32	Unstable	7.9	1.4	0.1	-0.5	0.1	6.2	Stable	0.3	-0.1	-0.1
RS33	Unstable	48.4	-3.4	-6.6	1.4	18.7	6.2	Unstable	-4.5	-6.6	1.8
RS34	Stable	3.1	-0.4	-1.6	-0.5	0.7	6.2	Stable	-1.4	-1.7	-0.1
RS41	Unstable	5.2	-5.9	-1.0	0.8	4.7	6.2	Stable	-6.7	-1.2	1.1
RS42	Stable	1.1	0.9	1.4	-0.3	0.5	6.2	Stable	0.2	1.2	0.0
RS43	Unstable	5.6	-4.7	-4.1	1.2	4.1	6.2	Stable	-5.1	-4.2	1.4
RS44	Unstable	18.5	1.6	-0.6	-0.7	0.7	6.2	Stable	0.8	-0.8	-0.3
RS51	Unstable	12.5	-3.0	0.2	1.3	9.3	6.2	Unstable	-3.9	0.0	1.6
RS52	Unstable	8.1	-1.0	1.3	-1.5	3.9	6.2	Stable	-1.9	1.1	-1.1
RS53	Unstable	7.3	0.5	-1.7	1.0	3.9	6.2	Stable	0.3	-2.0	1.1
RS54	Unstable	14.1	-1.0	3.6	-0.7	7.3	6.2	Unstable	-2.0	3.1	-0.3
RS61	Unstable	9.8	-3.1	1.6	1.2	6.6	6.2	Unstable	-4.0	1.4	1.6
RS62	Stable	0.7	-0.7	0.0	0.6	1.0	6.2	Stable	-1.2	-0.8	0.8
RS63	Unstable	5.5	3.1	2.6	2.0	3.3	6.2	Stable	2.9	2.0	2.0
RS64	Stable	0.8	-0.8	-1.9	0.3	0.8	6.2	Stable	-1.0	-2.1	0.5
RS71	Unstable	15.7	3.5	-2.0	-0.2	4.5	6.2	Stable	2.9	-2.3	0.1
RS72	Unstable	19.0	3.3	2.0	-0.2	4.9	6.2	Stable	2.8	0.9	-0.1
RS73	Unstable	9.2	0.2	0.6	1.3	3.7	6.2	Stable	0.1	-0.2	1.2
RS74	Unstable	7.8	2.6	1.2	-0.9	2.0	6.2	Stable	2.1	0.9	-0.6
RS81	Unstable	19.7	4.1	0.9	1.0	4.8	6.2	Stable	3.8	0.5	0.9
RS82	Unstable	138.1	2.0	2.8	0.1	2.9	6.2	Stable	1.4	1.7	0.2
RS91	Unstable	21.1	3.9	4.6	-0.3	7.9	6.2	Unstable	3.7	3.9	-0.2
RS92	Unstable	9.6	4.3	2.8	-0.2	5.0	6.2	Stable	3.8	1.5	-0.1

Points	Pelzer - Intensity of displacements [mm]					IWST- Intensity of displacements [mm]					
	Status	θ^2	dY	dX	dH	T	F	Status	dY	dX	dH
RS93	Unstable	40.3	5.4	7.4	0.5	15.4	6.2	Unstable	5.1	6.6	0.7
RS94	Stable	1.9	1.3	1.2	-0.4	0.7	6.2	Stable	0.8	0.0	-0.3



Sušić Z., Batilović M., Đurović R., Marković M., Vujinović M. (2023). Deformation analysis of Ratkov Laz bridge using Pelzer and IWST method. Geodetski vestnik, 67 (4), 487-504.

DOI: <https://doi.org/10.15292/geodetski-vestnik.2023.04.487-504>

Assoc. Prof. Zoran Sušić, Ph.D.

Faculty of Technical Sciences, University of Novi Sad
Trg Dositeja Obradovića 6, 21101 Novi Sad, Serbia
e-mail: zsušic@uns.ac.rs

Assoc. Prof. Marko Marković, Ph.D.

Faculty of Technical Sciences, University of Novi Sad
Trg Dositeja Obradovića 6, 21101 Novi Sad, Serbia
e-mail: marko_m@uns.ac.rs

Assist. Prof. Mehmed Batilović, Ph.D.

Faculty of Technical Sciences, University of Novi Sad
Trg Dositeja Obradovića 6, 21101 Novi Sad, Serbia
e-mail: mehmed@uns.ac.rs

Assist. Marijana Vujinović, M.Sc.

Faculty of Technical Sciences, University of Novi Sad
Trg Dositeja Obradovića 6, 21101 Novi Sad, Serbia
e-mail: marijana.petkovic@uns.ac.rs

Assoc. Prof. Radovan Đurović, Ph.D.

Faculty of Civil Engineering, University of Montenegro
Bulevar Džordža Vašingtona bb, 81000 Podgorica, Montenegro
e-mail: zlatko1979@yahoo.com